Composites Science and Technology 144 (2017) 223–229

Contents lists available at ScienceDirect

Composites Science and Technology

journal homepage: http://www.elsevier.com/locate/compscitech

Graphene oxide induced crosslinking and reinforcement of elastomers

Wang Xing [a], Hengyi Li [a], Guangsu Huang [a, ***], Li-Heng Cai [b, **], Jinrong Wu [a, *]

[a] State Key Laboratory of Polymer Materials Engineering, College of Polymer Science and Engineering, Sichuan University, Chengdu 610065, PR China
[b] John A. Paulson School of Engineering and Applied Sciences, Harvard University, Cambridge, MA 02138, USA

ARTICLE INFO

Article history:
Received 12 December 2016
Received in revised form
2 March 2017
Accepted 8 March 2017
Available online 8 March 2017

Keywords:
Polymer-matrix composites (PMCs)
Interface
Graphene oxide
Styrene-butadiene rubber

ABSTRACT

Conventional elastomer processing requires crosslinking elastomer using specific chemical reagents and reinforcing it using filler particles. Here we report a method to simultaneously crosslink and reinforce styrene-butadiene rubber (SBR) using graphene oxide (GO). We find that GO not only acts as an effective reinforcing filler, but also is capable of generating free radicals upon heating, enabling covalent crosslinking of SBR. Moreover, the interaction between GO surface and SBR polymers results in an interfacial layer in which the density of crosslinks increases towards to the GO surface, thus interfacial layer shows much slower relaxation dynamics than the bulk rubber. The unique role of GO allows GO/SBR nanocomposites to have better mechanical properties than SBR crosslinked with conventional sulfur or dicumyl peroxide. The concept of using GO as both a filler and crosslinking agent may enable the discovery of polymeric nanocomposites with exceeding mechanical properties.

1. Introduction

Uncrosslinked rubber behaves like a liquid and cannot support external load. Crosslinking results in the formation of a permanent polymer network, enabling rubber with elastic properties similar to that of a solid. However, the mechanical properties of crosslinked rubbers, such as styrene-butadiene rubber (SBR) and polybutadiene rubber (BR), are barely good enough for most practical applications [1–3]. It is required to reinforce the crosslinked rubbers using filler particles to make them practically useful. As a result, rubber processing requires introducing both crosslinking agents and filler particles. This process, however, is very tedious and energy consuming, as it takes a long time of mechanical mixing to ensure homogenous dispersion of crosslinking agents and filler particles in the rubber matrix. Moreover, special care must be taken when designing a crosslinking recipe; the chemical activity of curing reagents and the amounts of activator and accelerator that regulate the crosslinking rate must be carefully balanced. It is highly desirable to develop a method that enables crosslinking and reinforcement of rubbers through a one-step process.

To circumvent the difficulties during rubber processing, a possible strategy is to develop particles that have dual functions; such particles should not only act as fillers, but also be able to crosslink rubbers. However, conventional fillers including carbon black and silica cannot crosslink a rubber, as they are chemically inert [4]. Similarly, other fillers, such as organoclays, carbon nanotubes and graphene, cannot serve as crosslinking agents [5–14]. Unlike conventional fillers, surface treated nanoparticles that carry highly-reactive functional groups can react with a certain type of functional groups in the rubber matrix and thus allow the nanoparticles to be used as crosslinkers. Such nanoparticle-polymer reaction, however, is often chemically specific and only applies to particular reaction types; examples include Si-H/vinyl hydrosilylation, epoxy/carboxyl and amine/isocyanate reactions [15–19]. These reaction types are only associated with a particular type of polymer matrices. Unfortunately, the most used unsaturated rubbers do not belong to this category, as the unsaturated rubbers are typically crosslinked by free radical reaction [4]. Thus, it will be highly advantageous if a particle can not only act as fillers but also generate free radicals to induce chemical crosslinking of unsaturated rubbers.

Here we report a method to simultaneously crosslink and reinforce SBR using graphene oxide (GO). Unlike conventional inert fillers and surface-treated nanoparticles, GO not only can act as fillers, but also is capable of generating free radicals upon heating [20–24], enabling crosslinking of SBR. We find that GO/SBR nanocomposites exhibit better mechanical performance than conventional crosslinked SBR,

* Corresponding author.
** Corresponding author.
*** Corresponding author.
E-mail addresses: guangsu-huang@hotmail.com (G. Huang), lhcai@seas.harvard.edu (L.-H. Cai), wujinrong@scu.edu.cn (J. Wu).

http://dx.doi.org/10.1016/j.compscitech.2017.03.006
0266-3538/

evidenced by 4 times increase in the tensile strength. Moreover, unlike conventional crosslinked SBR that has a nearly constant elastic modulus above glass transition temperature (T_g), the storage modulus of GO/SBR nanocomposites decreases as the temperature increases. We explain this phenomenon by proposing a multi-scale relaxation mechanism for polymers in the interfacial layer near the GO surface; in this layer polymers closer to the GO surface have higher Tg due to higher crosslinking density.

2. Experimental section

2.1. Materials

Highly-purified graphite flakes with a lateral size of about 1 μm were purchased from Qingdao Ruisheng Graphite Company, China. SBR latex (21 wt% of SBR content) was kindly provided by Lanzhou Petrochemical Company, Petro China. Curing reagents and other reagents were of analytical grade and commercially available.

2.2. Preparation of graphene oxide

Graphene oxide was produced by Hummers' method from graphite flakes [25], and then dispersed in deionized water by ultrasonic-treatment. The suspension was centrifuged at 10000 rpm for 15 min to remove unexfoliated graphite.

2.3. Preparation of GO/SBR nanocomposites

We prepared GO/SBR nanocomposites by a latex mixing method. In this method, the above-mentioned aqueous GO suspension was diluted to 0.1 wt% and then subjected to bath sonication for 0.5 h. SBR latex was then mixed with a prescribed amount of aqueous GO suspension by mechanical agitating. The resulting mixture was co-coagulated with sodium chloride solution, and the solids were filtrated and washed repeatedly with deionized water and then vacuum dried in an oven at 70 °C for 48 h to obtain SBR nanocomposites. The GO/SBR nanocomposites were hot-pressed at 170 °C for different time periods to obtain different crosslinking densities. For comparison, SBR samples crosslinked with sulfur and DCP were also prepared. The crosslinking recipe for sulfur is SBR 100 phr, sulfur 1.75 phr, ZnO 4 phr, CZ 1 phr and stearic acid 2 phr; while the crosslinking recipe for DCP is SBR 100 phr and DCP 1.5 phr.

2.4. Characterization

Atomic force microscopy (AFM, MFP-3D from Asylum Research) was used to characterize the morphology of GO. GO aqueous suspension was deposited on a freshly cleaved mica wafer by spin coating. AFM images were obtained using a tapping mode under ambient conditions. Wide angle X-ray diffraction (WAXD) was performed on a Philips X'Pert Graphics & Identify with Ni-filtered CuK α radiation (λ = 0.154 nm) at a generator voltage of 35 kV and a generator current of 25 mA. Angle scanning was performed at a speed of 2.4°/min from 5° to 50°. Transmission electron microscope (TEM) was performed on a FEI Tecnai G2 F20 S-TWIN. Ultrathin sections were obtained using a Leica Ultracut UCT ultramicrotome with a diamond knife cooled by liquid nitrogen to −100 °C.

The crosslinking process was analyzed with an oscillating disc rheometer (ODR, Beijing Youshen Electronic Apparatus Factory, China). After pre-heating the discs of ODR to a temperature of 170 °C, 10 g of GO/SBR nanocomposites was inserted between the two discs and the torque was monitored as a function of time. Measurements of differential scanning calorimeter (DSC) were performed on a Q200 (TA instruments) at 10 °C/min. The weight of each sample was in the range of 5–7 mg.

The gel content and crosslinking density were determined by equilibrium swelling measurements. A piece of GO/SBR nanocomposite was immersed in toluene for a week to extract the sol fraction, during which the solvent bath was replaced with fresh toluene every day. Crosslink density was determined according to Flory-Rehner equation [26]:

$$\nu_e = -\frac{\ln(1-\nu_r)+\nu_r+\chi\nu_r^2}{\nu_s\left(\nu_r^{1/3}-\nu_r/2\right)} \quad (1)$$

where ν_r is the volume fraction of the crosslinked polymer swollen to equilibrium and ν_s is the solvent molar volume (106.2 cm^3/mol for toluene). $\chi = 6.53\times10^{-2}$ is the SBR-toluene interaction parameter [27]. The value of ν_r is obtained according to:

$$\nu_r = \frac{w_2/\rho_2}{w_2/\rho_2+(w_1-w_2)/\rho_1} \quad (2)$$

where w_1 is the weight of the swollen gel, w_2 is the weight of the gel after drying, and ρ_1 and ρ_2 are the densities of the solvent and the rubber, respectively.

The tensile tests were conducted on an Instron 5567 at room temperature with a cross-head speed of 100 mm/min. The specimen was a dumbbell shaped thin strip (20 × 4 × 1 mm). For each data point, five parallel measurements were carried out and the average value was taken; the error bar corresponds to standard deviations for five measurements. Dynamic mechanical tests were performed on a DMA Q800 (TA instruments) at a frequency of 1 Hz from −100 °C to + 30 °C by using a tensile mode at an oscillation amplitude of 20 μm. The heating rate was 3 °C/min. The dimensions of the rectangle sample strips were 50 × 10 × 1 mm.

X-ray Photoelectron Spectroscopy (XPS) measurements were performed on an XSAM800 (Kratos) using a monochromatic Mg Ka X-ray source radiation ($h\nu = 253.6$ eV) operated at 12 kV and 15 mA. Fourier transform infrared spectroscopy (FTIR) characterization was performed on a Nicolet IS 10 spectrometer using attenuated total reflection (ATR). Raman spectra were recorded from 100 to 4000 cm^{-1} on a LABRAM HR800 confocal micro-Raman spectrometer using a 532 nm ND:YAG laser. Electron spin resonance (ESR) measurements were carried out on a JES-FA200 instrument. The power and frequency of the microwave radiation were 1.0 mW and 9.4 GHz, respectively.

3. Results and discussion

We prepare GO/SBR nanocomposites by a two-step process that involves fabrication of GO and mixing GO with SBR afterwards. We fabricate GO using graphite according to the Hummers' method [25]. The GO has a thickness of ~1 nm and a lateral size of ~1 μm, as shown by the atomic force microscopy (AFM) image in Fig. 1a. We use a latex mixing method to homogeneously disperse GO in the polymer matrix without re-stacking. In particular, we mix surfactant stabilized SBR emulsion with a prescribed amount of aqueous GO suspension, and then add saturated NaCl solution to coagulate the mixture. The coagulated material is separated from the mixture, and washed using distilled water to remove the salt and surfactant, followed by vacuum drying. The dried material is further processed by a twin-roll milling that exfoliates the possibly re-stacked GO during coagulation and to promote homogenous distribution of GO in SBR [28,29]. Indeed, GO is homogenously distributed in the SBR matrix, as shown by the transmission electron microscopy (TEM) images in Fig. 1b and c. Moreover, the complete exfoliation of GO is further confirmed by wide angle X-ray diffraction measurements;

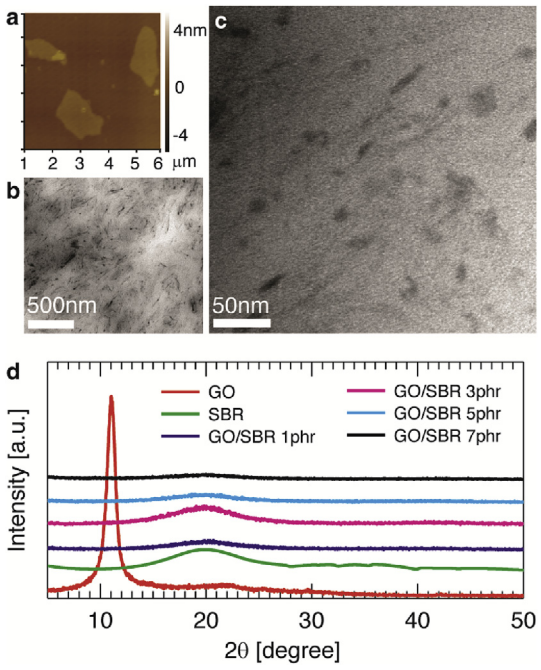

Fig. 1. Morphologies and structural characterization of graphite oxide and graphene oxide/styrene butadiene rubber (GO/SBR) nanocomposites. (a) An example atomic force microscope (AFM) image of GO. (b) An example transmission electron microscope (TEM) image of GO/SBR nanocomposite with 7 phr GO and (c) its zoomed-in visualization. (d) X-ray diffraction (XRD) patterns of graphite oxide (red), SBR (green), and GO/SBR nanocomposites with different amounts of GO: 1 phr (purple), 3 phr (cyan), 5 phr (blue), and 7 phr (black). (For interpretation of the references to colour in this figure legend, the reader is referred to the web version of this article.)

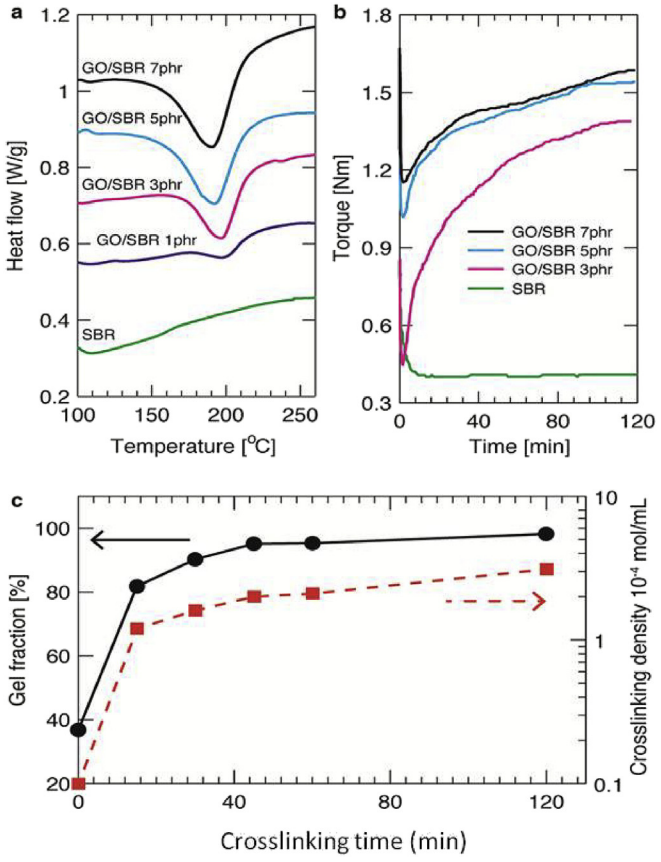

Fig. 2. Crosslinking SBR by GO. (a) Heat-flow curves of pure SBR and GO/SBR nanocomposites at a heating rate of 10 °C/min measured using differential scanning calorimetry (DSC). The curves are shifted vertically for clarity. (b) Curing curves of pure SBR and GO/SBR nanocomposites at 170 °C. (c) Gel fraction and crosslinking density as a function of crosslinking time for the GO/SBR nanocomposite with 3 phr GO.

unlike stacked GO that has a characteristic peak at $2\theta = 11.0^{\circ}$ due to the diffraction from multiple layers, this characteristic peak disappears in the GO/SBR nanocomposites, as shown by Fig. 1d.

Because chemical reactions usually generate or absorb heat, we use differential scanning calorimetry (DSC) to record the heat flow to test if GO can chemically react with SBR. In contrast to pure SBR that does not have any exothermic peaks, there are exothermic peaks between 190 °C and 200 °C for the GO/SBR nanocomposites, as shown in Fig. 2a. The exothermic peaks strongly suggest the existence of chemical reactions in the GO/SBR nanocomposites. However, it is possible that chemical reactions only occur within GO itself. Indeed, the DSC measurement for pure GO shows an exothermic peak at 210 °C because of thermal reduction (Fig. S1). Therefore, to determine if GO chemically react with SBR, we quantify the heat enthalpy of pure GO, and compare it with the heat enthalpies of GO/SBR nanocomposites; the heat enthalpy is defined as the energy corresponding to the exothermic peak and has a unit of Joule per gram GO (J/g_{GO}). Interestingly, we find that the heat enthalpies are 851 J/g_{GO}, 943 J/g_{GO} and 841 J/g_{GO} for GO/SBR nanocomposites with 3 phr, 5 phr and 7 phr GO, respectively; these values of enthalpies are higher than that of pure GO, 735 J/g_{GO}. Therefore, chemical reactions do occur between GO and SBR.

To test if the chemical reactions between GO and SRB result in the formation of a solidlike network, we characterize the curing process of the GO/SBR nanocomposites *in situ* using an oscillating disc rheometer (ODR). We sandwich a GO/SBR nanocomposite between the two discs of ODR that are preheated to 170 °C, and monitor the torque during the crosslinking process (Experimental Section). The temperature 170 °C is slightly below ~190 °C of the DSC exothermic peaks; this avoids rapid degradation of SBR under higher temperature. We find that initially the torque decreases due to lowered viscosity at elevated temperature, followed by a rapid increase upon crosslinking, and then saturates around the curing time of 120 min, indicating completion of the crosslinking, as shown in Fig. 2b; this behavior is reminiscent of conventional SBR crosslinking using sulfur or dicumyl peroxide (DCP), as shown in Fig. S2. The complete crosslinking is further evidenced by the large gel fraction and crosslinking density for the GO/SBR nanocomposites. After crosslinking at 170 °C for 120 min, the gel fraction for the GO/SBR nanocomposite with 3 phr GO is about 98% (wt/wt), slightly higher than 97.2% of sulfur crosslinked SBR and 94.6% of DCP crosslinked SBR, as shown in Fig. 2c. At the same time, the crosslinking density of the nanocomposite is 3.1×10^{-4} mol/cm^3, comparable to 3.2×10^{-4} mol/cm^3 of sulfur crosslinked SBR and 4.2×10^{-4} mol/cm^3 of DCP crosslinked SBR. Besides, the inclusion of GO provides additional entanglements, namely physical crosslinking, caused by π-π interaction between the double bonds on the rubber molecular chains and the GE nanoplatelets. In addition, there is no observable increase in torque for pure SBR, as shown by the green line Fig. 2b; this suggests that the crosslinking cannot happen within SBR itself. Collectively, our results demonstrate that GO acts as a crosslinking agent that enables formation of a solidlike network.

We next quantify the mechanical properties of crosslinked GO/SBR nanocomposites using tensile tests. The tensile strength of the GO/SBR nanocomposite with 3 phr GO increases monotonously with the crosslinking time, and saturates at crosslinking time 120 min with a value of 6.6 MPa; this value is more than 4 times of pure SBR crosslinked by either sulfur or DCP, as shown in Fig. 3a.

Moreover, at the crosslinking time 120 min, the tensile strain at break for the GO/SBR nanocomposite is 820%, noticeably larger than 530% of sulfur crosslinked SBR and 280% of DCP crosslinked SBR, as shown in Fig. 3b. Such a noticeable increase in both tensile strength and strain strongly suggest that GO not only crosslinks the SBR, but also reinforces the nanocomposites by acting as filler particles, resulting in much better mechanical properties.

To understand the dual-role of GO as both filler particles and crosslinking agents, we exploit the chemical structure of GO and its possibility to change upon heating. Unlike conventional fillers such as carbon black, GO contains oxygenic groups such as hydroxyls that may undergo homolytic cleavage at high temperature. The homolytic cleavage of oxygenic groups on GO generates two types of radicals; one is radicals carried by the oxygenic groups that can diffuse into the SRB matrix, whereas the other is localized on the surface of GO, as illustrated in Fig. 4a. We expect that both the two types of free radicals can induce crosslinking of SBR, similar to the crosslinking mechanisms of peroxides [4].

To verify that homolytic cleavage of oxygenic groups can occur at high temperature, we use X-ray photoelectron spectroscopy (XPS) to quantify the change of oxygenic groups for pure GO upon heating. Indeed, after 30 min at 170 °C, we find that the non-oxygenated carbon (284.6 eV) becomes more abundant, suggesting a decrease in weight fraction of carbon in other structural groups that include C—O bonds (286.1 eV), carbonyl groups (C═O, 287.6 eV) and carboxylate groups (O—C═O, 289.2 eV), as shown in Fig. 5a and b. This increase in the relative amount of ring carbon is partially due to homolytic bond breakage of C—OH and C—COOH bonds, which have relatively lower bonding energies (C—COOH, 348 kJ/mol; C—OH, 358 kJ/mol) compared to other single bonds and ring C—C bonds (C—H, 413 kJ/mol; O—H, 463 kJ/mol; ring C—C, 473 kJ/mol) [23,30,31].

To provide direct evidence to the generation of radicals by homolytic bond cleavage at high temperature, we perform electron paramagnetic resonance (EPR) measurements *in situ*. The EPR intensity is proportional to the concentration of radicals. Due to the upper temperature limit of EPR, we measure the intensity of EPR signal for pure GO at 140 °C. We observe a rapid increase in EPR signal within 13 min s, followed by a relatively slow increase at least up to 36 min s, as shown in Fig. 5c; this indicates a continuous production of radicals due to the cleavage of oxygenic groups on GO.

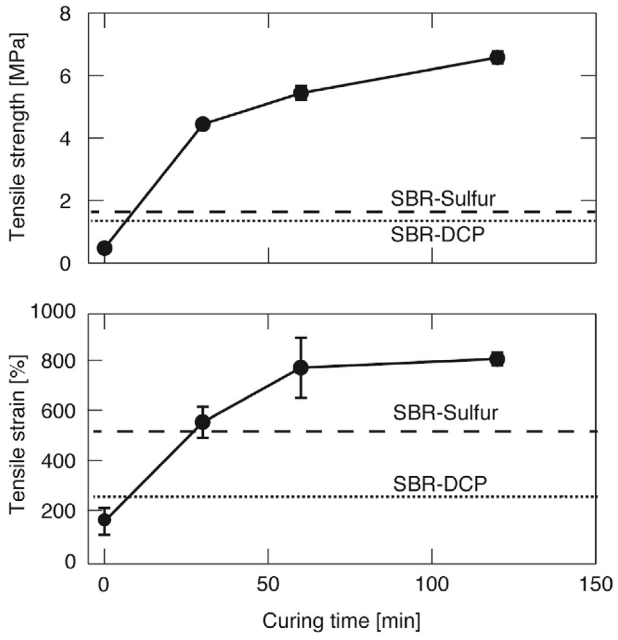

Fig. 3. Effect of curing time on the mechanical properties of GO/SBR nanocomposite with 3 phr GO. (a) Tensile strength; (b) tensile strain. The mechanical properties of SBR cured with sulfur (dashed line) and dicumyl peroxide (DCP) (dotted line) are also plotted for comparison.

The free radicals can either diffuse into the SBR matrix or locate at the interface between GO and SBR; both enables crosslinking of the nanocomposites. Indeed, the radical-induced crosslinking reaction are suggested by the change of two characteristic peaks of Fourier Transform Infrared Spectroscopy (FTIR): One peak at 1260 cm^{-1} disappears due to cleavage of phenol groups on GO, and the other peak at 1643 cm^{-1} becomes less pronounced due to the reaction of C═C bonds in SBR induced by the radicals [20,32], as shown in Fig. 5d. Collectively, our results demonstrate that homolytic cleavage of oxygenic groups in GO generates radicals that allow crosslinking of GO/SBR composites, as schematically described in Fig. 4.

In addition to producing free radicals that chemically crosslink SBR, GO can also physically interact with SBR polymers. The bound rubber content, which cannot be extracted by good solvents in the uncrosslinked nanocomposites, is about 37% (wt/wt) prior to crosslinking, as shown by the circle point on the left in Fig. 2c. Such noticeable bound-rubber content indicates a strong interfacial interaction originated from CH—π interactions between SBR and GO. To verify this interfacial interaction, we use FTIR measurements to detect the shifts of characteristic peaks of SBR. Pure SBR shows a CH_2 asymmetric stretching band at 2920 cm^{-1}, a CH_2 symmetric stretching band at 2851 cm^{-1}, a = C—H out-of-plane bending band at 966 cm^{-1} and an aromatic ring stretching at 1494 cm^{-1} [33]. Adding GO in SBR leads to charge transfer between C—H bonds on SBR and π electron on GO, which weakens C—H bonds [34,35]; as a result, the characteristic peaks of C—H bonds show red-shifts with shifting values ranging from 2 to 4 cm^{-1}, as shown in Fig. 6. By contrast, the aromatic ring stretching has no observable shifting, as shown in Fig. S3. Our observation collectively suggests that the CH—π interaction dominates the interfacial interaction between SBR and GO [34,35]. Moreover, we find that crosslinking further shifts the bands of C—H bonds toward lower wavenumbers, as shown in Fig. 6; this suggests the chemical bonds between SBR and GO can enhance the CH—π interaction.

Unlike chemical bonding, the physical interfacial interactions between polymers and GO are not permanent; instead they can dissociate to allow polymers to relax, and this relaxation can be accelerated at higher temperature. Based on this understanding, we thus exploit the viscoelastic properties of GO/SBR nanocomposites using dynamic mechanical analysis (DMA) at 1 Hz within a temperature range from −70 °C to 150 °C. Interestingly, we observe two regimes for the GO/SBR nanocomposites: at relatively low temperature from −50 °C to −10 °C, E' decreases dramatically by two orders of magnitude from ~10^9 Pa to ~10^7 Pa; at the temperature from −10 °C to 150 °C, E' exhibits a relatively slow yet noticeable decrease from 10^7 Pa to 10^6 Pa, as shown by the solid lines in Fig. 7a. This decrease for GO/SBR nanocomposites is in striking contrast to DCP crosslinked SBR, which shows a nearly constant E' from −10 °C to 150 °C. Moreover, we find a second high-temperature peak on the loss tangent (tanδ) curves, $\tan\delta = E''/E'$, for the GO/SBR nanocomposites upon temperature sweep; unlike the sharp, narrow tanδ peak around the glass transition for SBR crosslinked with DCP, this second peak is very broad, spreading from −10 °C to 150 °C, as shown in Fig. 7b. Both the slow decrease in E' upon temperature increase and the wide second tanδ peak indicate a wide distribution of relaxation time for the polymers physically or chemically adsorbed onto the GO surface.

The effects of interfacial interaction between polymers and GO

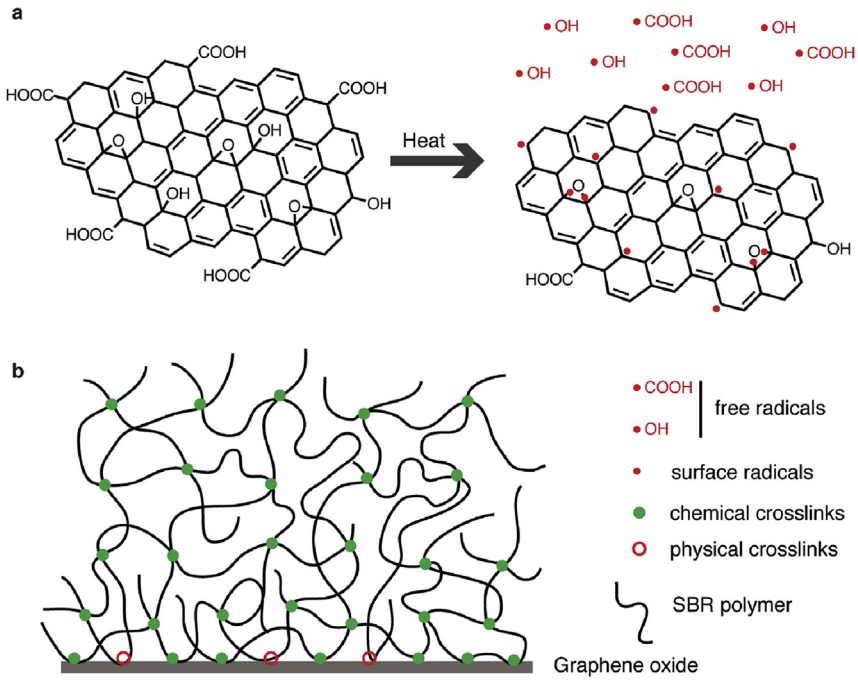

Fig. 4. A schematic description of the crosslinking mechanism of GO. The homolytic cleavage of oxygenic groups on GO produces two categories of free radicals, including free radicals on cleaved groups and free radicals on GO. The free radicals on the cleaved group can diffuse away from GO and lead to crosslinking of the rubber matrix; while the free radicals on GO are localized and result in interfacial crosslinking between GO and SBR. In addition to chemical crosslinks induced by free radicals, there are also physical crosslinks (empty circles) due to the absorption of polymers onto GO. The crosslinking density decreases as the distance from the GO surface increases, and eventually becomes a constant.

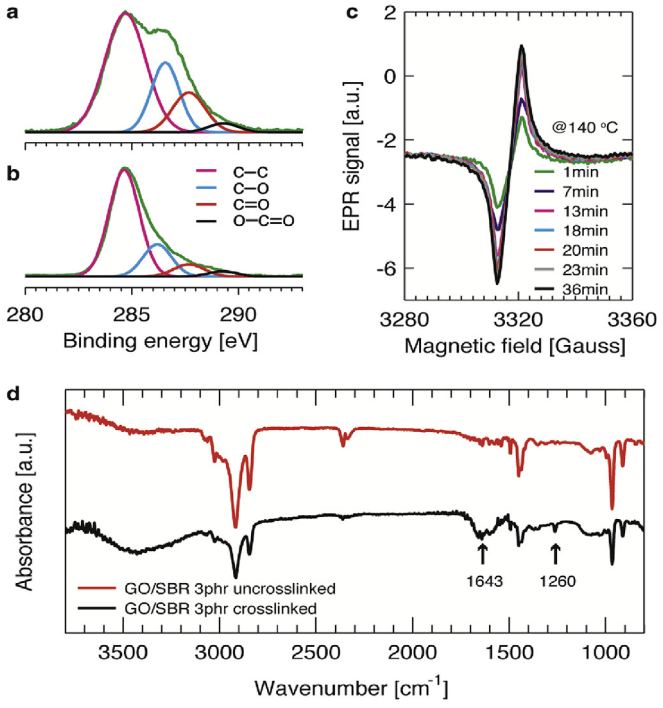

Fig. 5. Effect of thermal annealing on the chemical structure and free radicals of GO, and the chemical structure of GO/SBR nanocomposites. C 1*s* x-ray photoemission spectra (XPS) of (a) pristine GO and (b) GO after thermal annealing at 170 °C for 30 min. (c) Electron paramagnetic resonance (EPR) spectra of GO heated at 140 °C for different time. (d) Fourier transform infrared spectroscopy (FTIR) spectra of uncrosslinked (red line) and crosslinked (black line) GO/SBR nanocomposites with 3 phr GO; the crosslinking is performed at 170 °C for 2 h. (For interpretation of the references to colour in this figure legend, the reader is referred to the web version of this article.)

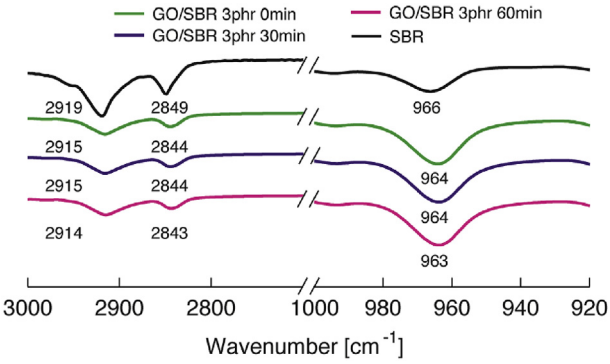

Fig. 6. Characterization on the interfacial interaction between SBR and GO. FTIR spectra of pure SBR and GO/SBR nanocomposite with 3 phr GO crosslinked at different time.

surface on the dynamic mechanical properties of GO/SBR nanocomposites can be qualitatively understood based on a multi-scale relaxation of polymers. The crosslinking of SBR not only happens in bulk polymer matrix because of diffusive free radicals, it also happens on the surface of GO due to the localized free radicals. Together with the free radical initiated chemical crosslinking on the interface, the physical CH-π interactions result in absorption of polymers onto the GO surface, as illustrated in Fig. 4. Both the chemical and physical interactions may render a surface coated with polymers forming a de Gennes' carpet-like structure [36], in which the effective crosslinking density increases towards the substrate surface, as illustrated in Fig. 4b. Because polymer networks of higher crosslinking density have higher glass transition temperature (T_g) due to reduced polymer mobility, the polymers closer to the GO surface are likely to have higher T_g [11,37–41]. Consequently, polymers in GO/SBR composites may adapt a multi-scale relaxation mechanism: As the temperature increases, the

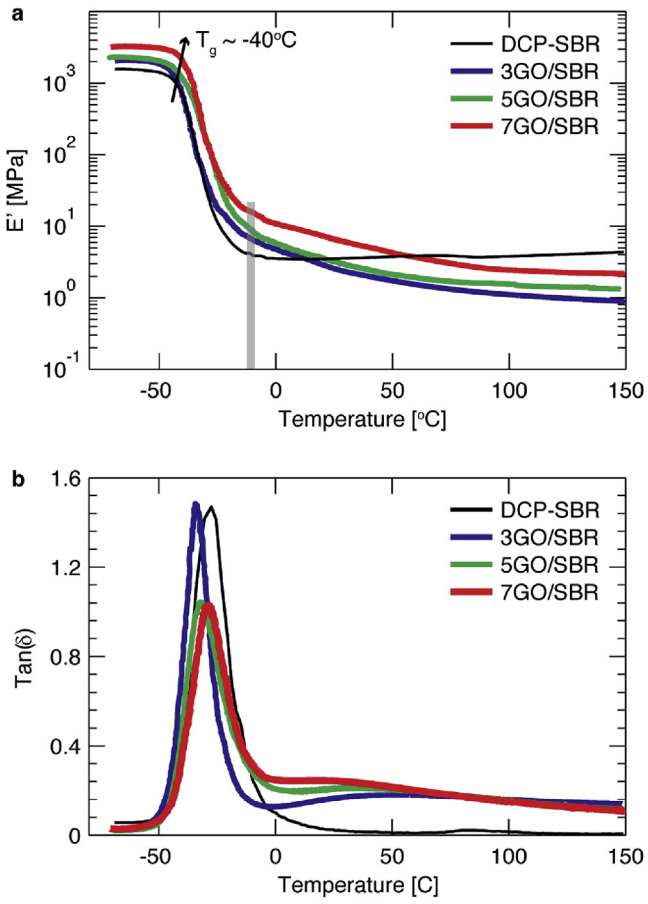

Fig. 7. Dynamic mechanical property. (a) Storage modulus (E') and **(b)** loss tangent ($\tan\delta$) as a function of temperature for DCP crosslinked SBR and GO crosslinked GO/SBR nanocomposites with different weight fraction of GO.

polymers far from the GO surface relax first, and followed by the relaxation of polymers closer to the GO surface. The multi-scale relaxation is reflected by the decrease in E' upon temperature increase and a second broad loss tangent peak at relatively high temperature, as evidenced by Fig. 7.

To roughly estimate the thickness of the restricted interfacial layer, we fit the $\tan\delta$ curve in Fig. 7b with an empirical model of asymmetric double sigmoid (ADS) proposed by Arrighi and coworkers [11], as discussed in the supporting information. We find that thickness values of the interfacial layer of GO/SBR nanocomposites with 3, 5 and 7 phr GO are about 13, 11 and 7 nm, respectively. A probable reason for the decreased interfacial thickness with increasing GO content is that some graphene layers may interact with each other and cannot be fully exposed to the rubber matrix at high GO loadings; this effect is not taken this into consideration during the calculation process, thus leading to overestimation of the GO surface area. However, these thickness values are much larger than that of many other nanocomposites, for example, 1 nm of carbon black and 2~5 nm of silica filled rubber nanocomposites [11,42–44]. This result suggests the interfacial interaction is stronger in the GO/SBR nanocomposites.

4. Conclusions

We have developed a method to simultaneously crosslink and reinforce rubbers using graphene oxide. Unlike conventional inert filler particles, graphene oxide not only reinforces the rubber by serving as fillers, but also is able to generate radicals that induce chemical crosslinking of the rubber. The mechanical properties of GO/SBR nanocomposites are better than that of rubber crosslinked by conventional methods; moreover, the properties can in principle be further improved by tuning the fraction of GO. Importantly, the existence of an interfacial layer between polymers and GO surface adds an additional dimension to the parameter space for tuning the properties of GO/SBR nanocomposites. However, quantitative understanding of the thickness for interfacial layer and its role in affecting the mechanical properties of the nanocomposites remain to be explored. Nevertheless, our system provides a model system to further explore the effects of interfacial layer on the mechanical properties of GO/rubber nanocomposites, which has been studied extensively for 3D spherical filler particles, yet to be investigated for 2D fillers such as GO. Finally, the concept of using graphene oxide as both filler particles and crosslinking agents may enable the discovery of polymeric nanocomposites with exceeding mechanical properties.

Acknowledgment

This work was financially supported by National Natural Science Foundation of China (grant No.: 51203096) and Sichuan University (grant No. 2013SCU04A01).

Appendix A. Supplementary data

Supplementary data related to this article can be found at http://dx.doi.org/10.1016/j.compscitech.2017.03.006.

References

[1] J.E. Mark, Polymer Data Handbook, Oxford University Press, New York, 1999.
[2] G. Heinrich, M. Kluppel, T.A. Vilgis, Reinforcement of elastomers, Curr. Opin. Solid State Mater. Sci. 6 (2002) 195–203.
[3] W. Xing, M.Z. Tang, J.R. Wu, G.S. Huang, H. Li, Z.Y. Lei, et al., Multifunctional properties of graphene/rubber nanocomposites fabricated by a modified latex compounding method, Compos. Sci. Technol. 99 (2014) 67–74.
[4] J.E. Mark, B. Erman, F.R. Eirich, Science and Technology of Rubber, third ed., Academic, New York, 2005.
[5] M.A. López-Manchado, M. Arroyo, B. Herrero, J. Biagiotti, Vulcanization kinetics of natural rubber–organoclay nanocomposites, J. Appl. Polym. Sci. 89 (2003) 1–15.
[6] M.A. López-Manchado, J. Biagiotti, L. Valentini, J.M. Kenny, Dynamic mechanical and Raman spectroscopy studies on interaction between single-walled carbon nanotubes and natural rubber, J. Appl. Polym. Sci. 92 (2004) 3394–3400.
[7] Z.H. Li, J. Zhang, S.J. Chen, Effects of carbon blacks with various structures on vulcanization and reinforcement of filled ethylene-propylene-diene rubber, Express Polym. Lett. 2 (2008) 695–704.
[8] J.R. Wu, W. Xing, G.S. Huang, H. Li, M.Z. Tang, S.D. Wu, et al., Vulcanization kinetics of graphene/natural rubber nanocomposites, Polymer 54 (2013) 3314–3323.
[9] Z. Tang, X. Wu, B. Guo, L. Zhang, D. Jia, Preparation of butadiene-styrene-vinyl pyridine rubber-graphene oxide hybrids through co-coagulation process and in situ interface tailoring, J. Mater. Chem. 22 (2012) 7492–7501.
[10] H. Kang, K. Zuo, Z. Wang, L. Zhang, L. Liu, B. Guo, Using a green method to develop graphene oxide/elastomers nanocomposites with combination of high barrier and mechanical performance, Compos. Sci. Technol. 92 (2014) 1–8.
[11] V. Arrighi, I. McEwen, H. Qian, M. Serrano Prieto, The glass transition and interfacial layer in styrene-butadiene rubber containing silica nanofiller, Polymer 44 (2003) 6259–6266.
[12] Y. Qiu, J. Wang, D. Wu, Z. Wang, M. Zhang, Y. Yao, et al., Thermoplastic polyester elastomer nanocomposites filled with graphene: mechanical and viscoelastic properties, Compos. Sci. Technol. 132 (2016) 108–115.
[13] Z. Yang, J. Liu, R. Liao, G. Yang, X. Wu, Z. Tang, et al., Rational design of covalent interfaces for graphene/elastomer nanocomposites, Compos. Sci. Technol. 132 (2016) 68–75.
[14] X. Ji, L. Cui, Y. Xu, J. Liu, Non-covalent interactions for synthesis of new graphene based composites, Compos. Sci. Technol. 106 (2015) 25–31.
[15] S. Sahoo, Polyhedral oligomeric silsesquioxane (POSS) nanoparticles as new crosslinking agent for functionalized rubber, Rubber Chem. Technol. 80((2007) 826–837.
[16] Q. Liu, W. Ren, Y. Zhang, Y. Zhang, Curing reactions and properties of

organic–inorganic composites from hydrogenated carboxylated nitrile rubber and epoxycyclohexyl polyhedral oligomeric silsesquioxanes, Polym. Int. 60 (2011) 422–429.
[17] H. Liu, S. Zheng, Polyurethane networks nanoreinforced by polyhedral oligomeric silsesquioxane, Macromol. Rapid Commun. 26 (2005) 196–200.
[18] D. Chen, S. Yi, W. Wu, Y. Zhong, J. Liao, C. Huang, et al., Synthesis and characterization of novel room temperature vulcanized (RTV) silicone rubbers using Vinyl-POSS derivatives as cross linking agents, Polymer 51 (2010) 3867–3878.
[19] Y. Shi, X. Gao, D. Zhang, Y. Liu, G. Huang, Synthesis and thermal properties of modified room temperature vulcanized (RTV) silicone rubber using polyhedral oligomeric silsesquioxane (POSS) as a cross linking agent, RSC Adv. 78 (2014) 41453–41460.
[20] J. Yang, M. Tian, Q.X. Jia, J.H. Shi, L.Q. Zhang, S.H. Lim, et al., Improved mechanical and functional properties of elastomer/graphite nanocomposites prepared by latex compounding, Acta. Mater. 55 (2007) 6372–6382.
[21] F. Beckert, A.M. Rostas, R. Thomann, S. Weber, E. Schleicher, C. Friedrich, et al., Self-initiated free radical grafting of styrene homo-and copolymers onto functionalized graphene, Macromolecules 46 (2013) 5488–5496.
[22] R. Feng, W. Zhou, G. Guan, C. Li, D. Zhang, Y. Xiao, et al., Surface decoration of graphene by grafting polymerization using graphene oxide as the initiator, J. Mater. Chem. 22 (2012) 3982–3989.
[23] X.L. Hou, J.L. Li, S.C. Drew, B. Tang, L. Sun, X.G. Wang, Tuning radical species in graphene oxide in aqueous solution by photoirradiation, J. Phys. Chem. C 117 (2013) 6788–6793.
[24] H. Xu, K.S. Suslick, Sonochemical preparation of functionalized graphenes, J. Am. Chem. Soc. 133 (2011) 9148–9151.
[25] W.S. Hummers, R.E. Offeman, Preparation of graphitic oxide, J. Am. Chem. Soc. 80 (1958), 1339–1339.
[26] P.J. Flory, Statistical mechanics of swelling network structures, J. Chem. Phys. 18 (1950) 108–111.
[27] A. Tager, Physical Chemistry of Polymers, Cornell University, New York, 1953.
[28] J.R. Potts, O. Shankar, L. Du, R.S. Ruoff, Processing–morphology–property relationships and composite theory analysis of reduced graphene oxide natural rubber nanocomposites, Macromolecules 45 (2012) 6045–6055.
[29] Y. Zhan, M. Lavorgna, G. Buonocore, H. Xia, Enhancing electrical conductivity of rubber composites by constructing interconnected network of self-assembled graphene with latex mixing, J. Mater. Chem. 22 (2012) 10464–10468.
[30] K. Erickson, R. Erni, Z. Lee, N. Alem, W. Gannett, A. Zettl, Determination of the local chemical structure of graphene oxide and reduced graphene oxide, Adv. Mater. 22 (2010) 4467–4472.
[31] X. Gao, J. Jang, S. Nagase, Hydrazine and thermal reduction of graphene oxide: reaction mechanisms, product structures, and reaction design, J. Phys. Chem. C 114 (2009) 832–842.
[32] M. Long, Y. Qin, C. Chen, X. Guo, B. Tan, W. Cai, Origin of visible light photoactivity of reduced graphene oxide/TiO2 by in situ hydrothermal growth of undergrown TiO2 with graphene oxide, J. Phys. Chem. C 117 (2013) 16734–16741.
[33] S. Munteanu, C. Vasile, Spectral and thermal characterization of styrene-butadiene copolymers with different architectures, J. Optoelectron. Adv. Mater. 7 (2005) 3135–3148.
[34] D. Baskaran, J.W. Mays, M.S. Bratcher, Noncovalent and nonspecific molecular interactions of polymers with multiwalled carbon nanotubes, Chem. Mater. 17 (2005) 3389–3397.
[35] W. Chung, K. Nobusawa, H. Kamikubo, M. Kataoka, M. Fujiki, M. Naito, Time-resolved observation of chiral-index-selective wrapping on single-walled carbon nanotube with non-aromatic polysilane, J. Am. Chem. Soc. 135 (2013) 2374–2383.
[36] P.G. De Gennes, Scaling Concepts in Polymer Physics, Cornell university, 1979.
[37] P. Rittigstein, R.D. Priestley, L.J. Broadbelt, J.M. Torkelson, Model polymer nanocomposites provide an understanding of confinement effects in real nanocomposites, Nat. Mater. 6 (2007) 278–282.
[38] T. Ramanathan, A.A. Abdala, S. Stankovich, D.A. Dikin, M. Herrera-Alonso, R.D. Piner, et al., Functionalized graphene sheets for polymer nanocomposites, Nat. Nanotechnol. 3 (2008) 327–331.
[39] K.H. Liao, S. Kobayashi, H. Kim, A.A. Abdala, C.W. Macosko, Influence of functionalized graphene sheets on modulus and glass transition of PMMA, Macromolecules 47 (2014) 7674–7676.
[40] K.H. Liao, S. Aoyama, A.A. Abdala, C. Macosko, Does graphene change Tg of nanocomposites? Macromolecules 47 (2014) 8311–8319.
[41] X. Li, J. Warzywoda, G.B. McKenna, Mechanical responses of a polymer graphene-sheet nano-sandwich, Polymer 55 (2014) 4976–4982.
[42] V. Arrighi, J.S. Higgins, A.N. Burgess, G. Floudas, Local dynamics of poly(-dimethyl siloxane) in the presence of reinforcing filler particles, Polymer 39 (1998) 6369–6376.
[43] V. Litvinov, P. Steeman, EPDM-carbon black interactions and the reinforcement mechanisms, as studied by low-resolution 1H NMR, Macromolecules 32 (1999) 8476–8490.
[44] V. Litvinov, R. Orza, M. Kluppel, M. Van Duin, P. Magusin, Rubber–filler interactions and network structure in relation to stress–strain behavior of vulcanized, carbon black filled EPDM, Macromolecules 44 (2011) 4887–4900.